SAKARYA UNIVERSITY
OF APPLIED SCIENCES

Skeletal Muscle Mechanics from Hill-Based Muscle Model to Computer Applications: State of the Art Review

Hamid ASADI DERESHGI [1] , Kasim SERBEST[2*] , Sema Nur SAHIN[1], Busra BALIK[1]

[1] Department of Biomedical Engineering, Istanbul Arel University
[2] Department of Mechatronics Engineering, Sakarya University of Applied Sciences

ABSTRACT

The first studies on muscle mechanics widely accepted in the literature have been known the macroscopic mechanical behavior of skeletal muscle since 1920's. A. V. Hill and his associates used modern experimental equipment to understand muscle contraction. On the other hand, A. F. Huxley presented cross-bridge models to understand the mechanisms of molecular contraction level, thermodynamics and biochemical experiments on skeletal muscles in the 1950's. By the 1990's, computer applications have been used for analysis of muscle mechanics. In this way, some software such as OpenSim, LifeModeler and AnyBody have been developed for only mechanical analysis of musculoskeletal system. In addition, some software developed for general analysis of dynamic systems such as MATLAB, ADAMS, COMSOL and ANSYS can be used for analysis of muscle mechanics. In this study, Hill-type muscle model and Huxley-type cross-bridge model have been explained and computer applications of muscle mechanics have been mentioned.

Keywords: Muscle contraction, muscle force, joint moment, simulation model, finite element model

1   Introduction

Muscles can be defined as biochemical machines that convert chemical energy into mechanical energy. The movement of the links occurs as a result of the interaction of skeletal muscles, nervous system, bones and joints. During movement force generation is provided by skeletal muscles. Actin and myosin fibers in muscles produce force by controlling muscle contraction [1].

As a result of a good understanding of muscle contraction, improving training techniques, examination of muscle injuries, artificial links, and artificial muscles could be produced. There were two common theories about muscle contraction. The first case of this theory was the Hill muscle model (see Figure 1) proposed by A. V. Hill [2,3]. As a result of experimental studies of Hill especially on the sartorius muscle of the frog, the basic mechanical properties of muscle contraction were described. Hill-type muscle model explained the macro properties of muscles. The second common theory of muscle contraction is the sliding filament or cross-bridge theory proposed by Huxley [4,5]. This theory explained muscle contraction along with molecular bases. Thus, it also expressed the micro properties of the muscles. Figure 2 shows a schematic representation of the cross-bridge model. Here, the process from 0 to 5 referred to the mechanism of muscle contraction which was formed as a result of the cross-link between actin and myosin fibres.

Both the Hill-type muscle model and sliding filament theory were based on complex mathematical equations. Additionally, there were many parameters in the equations that should be determined

---

* Corresponding Author's email: kserbest@subu.edu.tr

experimentally. This made it difficult to use models in the study of muscle mechanics. Therefore, researchers in the study of muscle mechanics benefited greatly from computer simulations. This paper included studies based on computer simulations that had been performed to study muscle mechanics, especially since the 1990s. Studies on humans and animals reviewed separately. Moreover, the results of experimental studies are also mentioned.
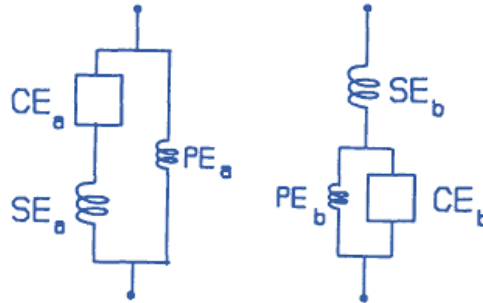

Figure 1: Classical structures for the Hill-type muscle model. CE; contractile element, SE; series element, PE; parallel element [6]
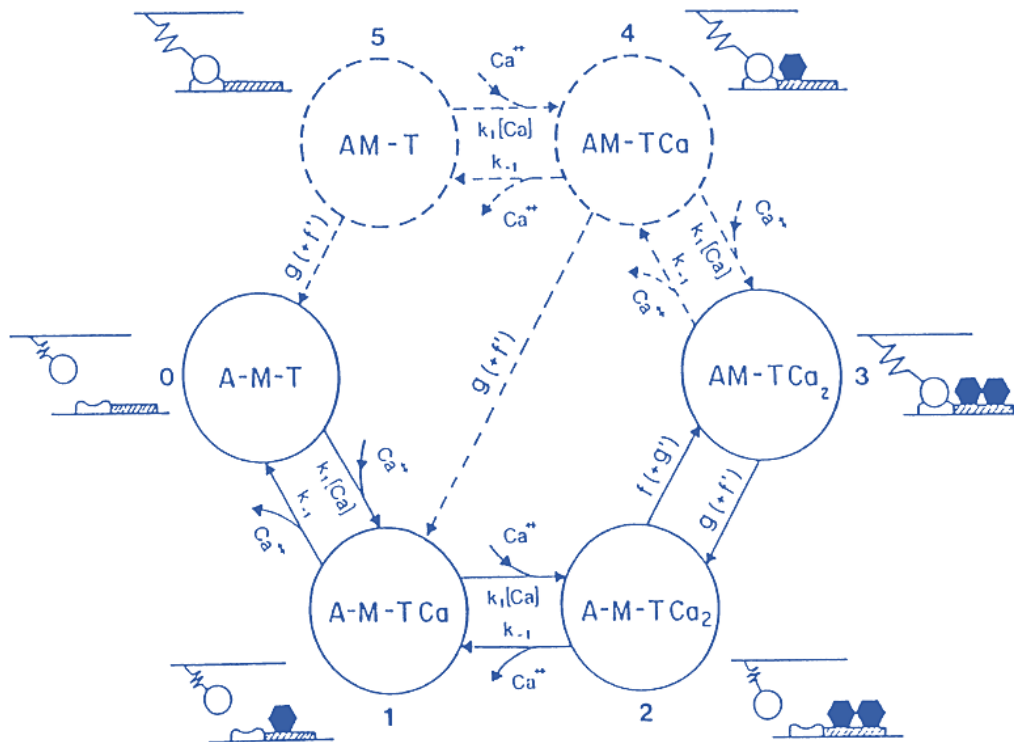

Figure 2: Kinetic diagram of the cross-bridge model. A; actin, M; myosin, T; troponin [6]

2 Human Studies

2.1 Studies for Skeletal Muscle

Chao et al. (1993) with the help of computers performed software and database that could be used in 3D to simulate the structures of muscles, skeletons, joints, ligaments, bones, and tendons of humans. As the analysis of the force of the exercised tissue could be done simultaneously with the exercise, they concluded that this software and database could be used in the treatment of musculoskeletal diseases [7].

Johansson et al. (2000) modeled muscle using a nonlinear continuous mechanical method. The purpose of this study was that the muscle and modeled in such a way that could be used in programs using the finite element method. In the results, they observed that this model could be used to define many muscle

characteristics and could also be included in the ANSYS program. Therefore, they concluded that this model can help solve many biomechanical problems [8].

Zhao and Narwani (2005) designed a reliable human body model for research and development applications of the safety system. Based on the integration of finite element models of specific areas of the body, they performed a finite element model of the human body for an adult male. Model's Post Mortem Human Subject (PMHS) responses to frontal and side blows under 15-35 MPH intensity were performed appropriately [9].

Martinek et al. (2008) proposed to develop a new approach to stimulate simulations such as Hodgkin-Huxley and to study fiber responses due to changes in its parameters. They calculated the changes concerning space and time with differential equations in the local Hodgkin-Huxley model and the equations in Hodgkin-Huxley spatial model. Using the bidomain model, extracellular potential distribution in the tissues around the fiber and intracellular potential distribution within the fiber were considered. They simulated static and time-dependent behaviours by performing 1, 2, and 3-dimensional models with COMSOL Multiphysics program. They compared the simulation results of the model performed with their new approach by comparing them with real data. In the evaluation of Hodgkin-Huxley-like stimulation processes, they concluded that the successful model was adaptable not just to fibers also with different geometries and parameters of extracellular regions [10].

Bai et al. (2008) constructed an analytical model of the musculoskeletal system of a complete male structure and a finite element model of the skeletal system. They had developed the CryoSegmentation software for the analytical model. It was observed that the dynamic of the resulting system will help to solve the mechanical nature of many biomechanical diseases by benefiting from the kinematic analysis [11].

Lu et al. (2010) used the finite element method to develop a three-dimensional visco-hyperelastic skeletal muscle model based on the Helmholtz free energy function. Using LS-DYNA simulation software, they analyzed the performance of the model, which was used to describe the under tension behavior of skeletal muscles. As a result of the elongation tests; the visco-hyperelastic behavior of both passive and active skeletal muscle tissues of the model could be simulated under high-stress rates of 10/s and 25/s, this was copatible with the simulation results obtained by the finite element method of experimental studies in the literature [12].

Kocbach et al. (2011) analyzed the equipment performance in termostimulation of muscle tissue by performing its optimization, also they determined the changing design parameters and different heating methods of thermostimulation equipment by calculating the temperature and electric field distribution in the body tissue according to the changing body composition. They carried out simulations using COMSOL Multiphysics to determine the optimized conditions and parameters. They observed that with microwave heating which was one of the approaches taken for heating biological tissue, the steady-state temperature reached faster than conventional and infrared heating and that a higher temperature could be achieved by heating the muscles directly. They suggested in electrical muscle stimulation for the administration of stimulation current using two contact points at the same end of the electrodes, an electrode conductivity of 40 S / m or higher should be used. They concluded that even higher electrode conductivity should be used for longer electrodes using two contact points on the same end [13].

Trinler and Baker (2018) found a general method that could be used to examine the calibration of musculoskeletal models using inverse kinematics and to test Gait2329 specific to the OpenSim model. In this model, for the calibration process, three-step approach was adopted: scaling, fitting, and model marker localization without user intervention. According to the results obtained they observed that this approach was the general method for their purpose [14].

2.2 Upper Extremity

2.2.1 Experimental Studies

Lieber et al. (1990) by measuring the architectural features of the forearm muscles, they determined the degree of specialization of muscles and the effects of specialization on tendon transfer procedures. With the architecture of the wrist flexor and extensor muscles; they determined the muscle length and mass, fiber length and holding angle relative to the force generation axis of muscle fibers orientation,

DERESHGI et al.

Skeletal Muscle Mechanics from Hill-Based Muscle Model to Computer Applications: State of the Art Rev...

sarcomere length, physiological cross-sectional area, they also measured the diffraction angle using laser diffraction techniques and with the help of a photodiode array interfaced to the computer. They analyzed the obtained data using BMDP software. They also observed that wrist flexors had more cross-sectional area than extensors and it was bigger, they also observed that it created more tension [15].

Lieber et al. (1994) to determine the relationship between the length of the sarcomere of the extensor carpi radialis brevis muscle in the wrist and the joint angle, measured sarcomere length using laser diffraction and electron micrographs of muscle biopsies in full flexion, neutral, and full extension conditions to determine the relationship between the length of the sarcomere of the extensor carpi radialis brevis muscle in the wrist and the joint angle. They concluded that passive sarcomere lengths varied between 2.6 μm - 3.4 μm and active sarcomere lengths were between 2.44 μm - 3.33 μm over the entire range of ankle joint motion [16].

Rotter et al. (2002) investigated the change of biomechanical and biochemical properties of septal cartilage depending on age. Thus, they were able to set the standards for materials used for soft tissue replacement. After testing in limited compression to determine the balance modulus and hydraulic permeability, they analyzed the content of glycosaminoglycan and hydroxyproline. They observed that as the age of the donor increased, the equilibrium modulus and glycosaminoglycan content decreased, and the hydraulic permeability and hydroxyproline content increased [17].

Lehtinen et al. (2003) developed a reliable method using shoulder MRI images to measure and quantitative evaluation of the rotator cuff muscle mass in a shorter time. In the first method, they identified sections on a single Y-shaped image, and in the second method, they computed the cross-sections from two views. With the two methods they used, compared their results with the volume determined by the multi-image reconstruction method, eventually they concluded that the second method was more compatible. They also observed that the intraobserver and interobserver variability of the first method was 3.9% and 2.9%, while the second method varied 3.0% and 1.7%, respectively [18].

Mochizuki et al. (2008) examined the humeral joint of the supraspinatus and infraspinatus macroscopically to explain the rupture of the rotator cuff. In the results, it was observed that the anteroposterior footprint of the infraspinatus was longer than known and its average was 32.7 mm and the footprint of the supraspinatus was observed to be shorter than known, on average 12.6 mm. Consequently, they concluded that the rupture of the rotator cuff was caused more by infraspinatus because the infraspinatus was larger than known [19].

Li et al. (2018) investigated the effect of diabetes mellitus (DM) on intrinsic muscle stimulation and dynamic order between muscles during sensitive cramps (stable and unstable conditions). In the study, abductor pollicis brevis (APB) by recording the first dorsal interosseous (FDI) surface electromyographic (sEMG) signals were analyzed by cross-recursion quantification analysis (CRQA) method. Consequently, they achieved that the getting power of the patient and control groups was almost the same but in the patient group the neuropathic symptoms were higher and the motor and sensory nerve conduction velocities along the median nerve were higher compared to the control group [20].

Zilov et al. (2018) studied the chaotic dynamics of muscle biopotentials under different static loads, which is a result of the control of the motor cortex, they also analyzed electromyogram (EMG) results measured based on muscle movements. They compared the analyzed EMGs in pairs using the Wilcoxon test. Hereby, they proved the statistical instability of EMGs for voluntary and involuntary conditional movements obtained sequentially within the framework of the Eskov-Zinchenko effect [21].

Zhang et al. (2020) analyzed the dynamic coordination of eight upper extremity muscles during pinching and firm grip, via recorded EMG signals and using the multiplex replication network (MRN) with maximal voluntary contractions for low (30%), medium (50%) and high (70%) strength levels. The study concluded that based on the synergy between multiple muscles according to their strength levels, the coordination of the outer muscles is more suitable for force generation. Additionally, the coordination increases in the outer muscles as the strength is increased, but there is no change in the inner muscles [22].

DERESHGI et al.

Skeletal Muscle Mechanics from Hill-Based Muscle Model to Computer Applications: State of the Art Rev...

2.2.2 Modelling and Simulation Studies

Lieber (1993) provided a definition of basic muscle function, muscle structure, functional results, and its applicability to surgical procedures involving skeletal muscles. He emphasized that the length-tension relationship for isometric contractions and the force-velocity relationship for isotonic contractions are important in defining the mechanical properties of skeletal muscle. Furthermore, the amplitude of active muscle force production is determined by the length of muscle fiber also maximum muscle strength is determined by physiological cross-section. In this study, it was emphasized that in order for donor and recipient muscles to be compatible in surgical tendon transfer, the architectural features should be similar to each other and therefore the musculoskeletal system design studies should be further developed [23].

Lee et al. (1999) using metamorphosis and vision techniques simulated realistically plastic surgery operations through 3D face models from a specific photograph and designed morphing operators for this. They using the feature-based volume conversion technique performed a generic face model, determined human faces from photographs, recorded face modes, and with the metamorphosis used to transform one image into another reconstructed the three-dimensional face model. As a result of the study, although successful eye reconstruction could not be achieved, they performed acceptable facial models for surgery [24].

Teran et al. (2005) using the degenerate and reversible finite element method performed an upper extremity musculoskeletal model to bring a new approach to musculoskeletal models. From the perforeded model, they concluded that it allows geometric structures to be shown accurately, directionally, and heterogeneously [25].

Holzbaur et al. (2005) developed a three-dimensional model that includes all the major muscles of the upper extremity and characterizes the mechanical motion to simulate musculoskeletal surgery. This model provides an accurate estimation of muscle moment in a wide range of postures and can determine muscle strength according to the muscle activation model. The moment arms and maximum moment-generating capacity of each muscle group were tested against experimental data. They observed that this model is largely consistent with the literature describing isometric joint moments for each joint and shows the relationship between the joints [26].

Blemker et al. (2005) developed a 3-dimensional muscle model to determine the architecture of the biceps brachii muscle that is effective in tension and the causes of non-uniform tension. They performed a finite element model that covers the main features of the female internal geometry, simulates the conditions, and compares the tissue tensions performed in the model within vivo data. They concluded that along-fiber stretch varied from 1.0 to 1.6, the along-fiber shear strains are from 0.0 to 2.4 and the cross-fiber shear strains are from 0.0 to 0.5. They observed that along-fiber shear strains during aponeurosis are highest and cross-fiber shear strains are highest at the site where the fascicles enter aponeurosis [27].

Rehorn and Blemker (2010) performed a finite element model with magnetic resonance (MR) images and simple models of the biceps femoris long head (BFLH) muscle using Mimics segmentation software. Using an MRI-based model, we can determine the effect of location on stress injury in BFLH muscle, the effect of the width, thickness, and length of the aponeurosis of the BFLH muscle studied using simple models. As a result of the findings, when a muscle was divided into three areas, they found that the middle part with the most uneven stretches was related to the injury and used this part in the study. While the effect of thickness and length of aponeurosis on stress was negligible, reducing the width of aponeurosis to 80% led to a 60% increase in stress [28].

Silva et al. (2011) presented a muscle fatigue model based on the strength generation history of each muscle to predict the health level of a muscle and could work with Hill-type muscle models. They tested this model in the context of inverse dynamic analysis for the elbow joint and observed fatigue results for the brachialis muscle. Within the scope of forwarding and inverse dynamic analysis, while simulating muscle strengths in the presence of muscle fatigue, they concluded that it was computationally applicable to any existing multibody methodology [29].

DERESHGI et al.

Skeletal Muscle Mechanics from Hill-Based Muscle Model to Computer Applications: State of the Art Rev...

2.3 Lower Extremity

2.3.1 Experimental Studies

Stäubli et al. (1999) analyzed the mechanical tensile properties of quadriceps tendons and patellar ligaments. In the study carried out using the harvesting technique and uniaxial tensile fracture tests; the mean cross-sectional areas were 64.6 ± 8.4 mm^2 for the unconditioned quadriceps tendon and 61.9 ± 9.0 mm^2 for the preconditioned quadriceps tendon, 36.8 ± 5.7 mm^2 for the unconditioned patellar ligament, and 34.5 ± 4.4 mm^2 for the preconditioned patellar ligament. The mean values of final tensile stress (53.4 ± 7.2 mm^2) of unconditioned patellar ligaments were higher than the values of the unconditioned quadriceps tendon (33.6 ± 8.1 mm^2). They concluded that the elastic modulus of the preconditioned patellar ligaments was higher than that of the quadriceps tendons [30].

Bayraktar et al. (2004) compared the elastic and yield properties of femoral cortical and trabecular bone structure by mechanical tests and nonlinear finite element method. In the results according to the trabecular tissue, the average elastic structure of the cortical tissue was 15%, the stress efficiency was 17%, the stress efficiency was 27%, while the yield strength as they observed was close. They concluded that the cortical bone was approximately 25% stronger with the cumulative effect of the analyzed differences [31].

Ward et al. (2009) investigated 27 muscles to perform a data set that described architectural features of lower link muscles with high accuracy by characterizing the length of muscle fiber and the muscle's capacity to generate excursion and force. Using scanners, they obtained high-resolution MR and CT images of the samples. As a result of the study and according to its architectural features, soleus, gluteus medius, and vastus lateralis were the strongest muscles; the muscles with the greatest excursion were sartorius, gracilis, and semitendinosus. Plantarflexors, knee extensors, and hip adductors were of the strongest muscle groups; and those with the greatest excursion were hip adductors and hip extensors [32].

Alexander and Schwameder (2016) investigated the joint strengths of the lower extremities while walking on inclines of different degrees. To calculate lower extremity joint strengths transferred the obtained data to the Anybody Modeling System and analyzed the results using a standard model in the software. During downhill walking; compression forces of the hip, tibiofemoral and patellofemoral joints increased, ankle joint compression forces decreased, and all lower extremity joint forces increased with increasing inclination during uphill walking. In addition; they concluded that uphill walking might be more stressful for the hip and ankle joints, and downhill walking might be more stressful for some knee joint structures [33].

Alexander and Schwameder (2016) analyzed the effects on muscle strength change during the hike on different slopes in the muscles of the lower extremities (hip, tibiofemoral, patellofemoral, and ankle). They used the musculoskeletal model for analysis and the AnyBody modeling system to calculate muscle strength. The experiment was carried out with inclinations of $\pm 0°$, $\pm 6°$, $\pm 12°$, $\pm 18°$ at a speed of 1.1 m/s. According to the data obtained the change in quadriceps, gastrocnemii, and hamstring muscles in straight walking compared with downhill and uphill walking were as follows: in uphill 140% increase, 22% decrease, 22% decrease and in downhill 96%, 36%, 12% increase, respectively were observed [34].

Trinler et al. (2019) compared the AnyBody and OpenSim approaches for modeling, applied a t-test in MATLAB by analyzing the muscle strength analysis and the dynamic structure of the joint in both ways during walking. According to the results the two systems were compatible with each other, however, they observed differences in the sagittal ankle, hip angles, and sagittal knee moments for reasons such as joint descriptions or model marker placement [35].

2.3.2 Modelling and Simulation Studies

Brekelmans et al. (1972) simulated the femoral bone in 2D and 3D using the finite element method. According to results, they concluded that it is advantageous to use FEM in the representation of complex structures, such as changing the shape of the structure, changing the force, or representing the model in 3 dimensions [36].

DERESHGI et al.

Skeletal Muscle Mechanics from Hill-Based Muscle Model to Computer Applications: State of the Art Rev...

Delp et al. (1994) for the treatment of patients with cerebral palsy, identified the tendon that provided the best range of knee range after transfer so, in the surgical intervention, the differences between the four tendons (semitendinosus, gracilis, sartorius, iliotibial) investigated to determine the rectus femoris can be transferred or not. For this, they simulated the rectus femoris after surgery, using the OPTOTRAK/3010 digitizing system. They observed that there were differences between the transfer of the four tendons and the semitendinosus tendon gave the best results at 4-5 cm knee flexion [37].

Anderson (1996) studied case examples using rapid prototyping to demonstrate the impact of rapid prototyping on personal or pre-operative planning. As seen in the samples of this study, for the first time thanks to personal prototyping, a suitable implant was performed for the patient, and because of the prototype that was given to the surgeon before surgery, the surgery was performed more successfully. In other words, it was observed that rapid prototyping could be very useful in the medical field [38].

Godest et al. (2002) using the finite element method (PAM-SAFETM code), examined the stress at the knee joint, which was fabricated of polyethylene. They analyzed the static and kinematic stresses with a 3D model and compare them with experimental results. They observed that in all of the results internal and external rotations were greater than the experimental results of 1 - 1.5°, while other data were consistent with the experimental data [39].

Helwig et al. (2006) analyzed the behavior of the proximal femoral fracture using the finite element method (FEM) examined the explainability of models that could not reach the desired result in clinical practice with FEM. The findings concluded that it helped to understand the changes in clinical studies, but the model should be developed with various implants such as gamma nails and sliding nails to fully explain the effects [40].

Cilingir et al. (2007) analyzed the stress distribution and surface touch functioning of the hip joint, using the finite element method (FEM). They compared the 3-dimensional anatomical model with the three-dimensional and two-dimensional axially symmetric models for contact functioning and stress distribution analysis. According to the results, the difference between the same (3D) and different size (3D and 2D) models compared for contact mechanics were approximately 0.5% and 0.7%, respectively. Due to the observed small differences and faster running, they concluded that it was appropriate to use FEM for contact processing. However, they concluded that it would be appropriate to use a 3D analytical model as the comparisons of the obtained results on stress distribution were different from each other [41].
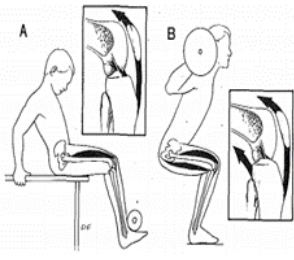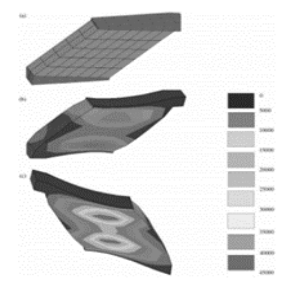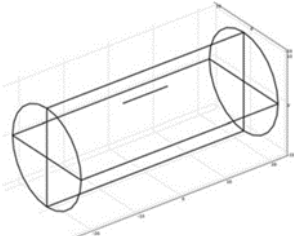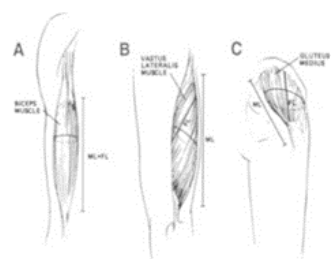
Linder-Ganz et al. (2007) calculated the tension and stress distribution in deep muscle and adipose tissues during sitting, depending on the mechanical conditions combined open-MR imaging and finite element modeling, and used SolidWorks for modeling using a reverse engineering approach. They found the maximum primary compressive tension and stress in the gluteus muscle 74% ± 7 and 32% ± 9 kPa, respectively, the maximum principal compressive tension and the stress surrounding the adipose tissue as 46 ± 7% and 18 ± 4 kPa, respectively. As a result of the finite element analysis, they observed that the maximum tissue tension and stress occurs in the gluteal muscles, not in the fat, ie close to the skin [42].
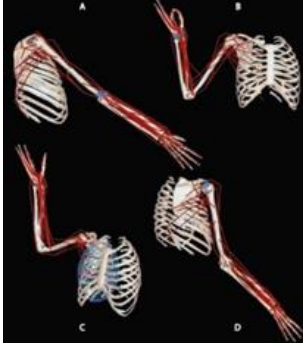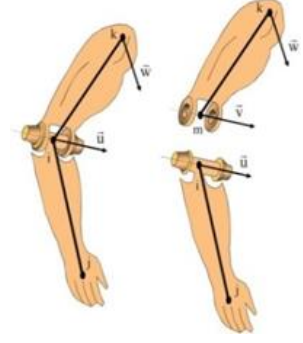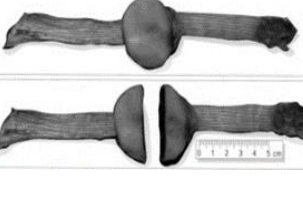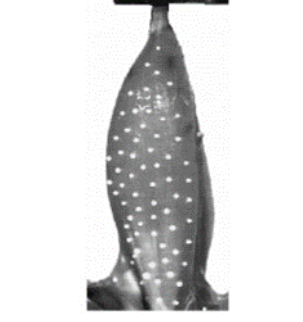
Carbone et al. (2016) performed a comprehensive sensitivity analysis to evaluate the effects of possible errors in Hill-type muscle-tendon model parameters for each of the 56 muscle tendons found in the musculoskeletal model. They simulated a lower extremity model in the AnyBody, to explain the functionality of the musculoskeletal system correctly. During a simulated walking cycle, they used the Local Sensitivity Index and the General Sensitivity Index measurements to distinguish the effect of the perturbation on the predicted force produced by the disrupted muscle-tendon fragments and all remaining muscle-tendon fragments. They observed that the sensitivity of the model was dependent on the size and length of the muscle-tendon segment as well as the specific role of each muscle-tendon segment during walking. The most sensitive parameter was tendon loose length, followed by maximum isometric muscle strength and optimal muscle fiber length parameters, they concluded that the nominal streamer angle showed very low sensitivity [43].

Żuk et al. (2018) examined the effect of variability of certain lower extremity musculoskeletal model parameters on muscle strength with inverse dynamics-based static optimization and hybrid approach compared various muscle models using OpenSim 3.0.1, one of the simulation software. They concluded

DERESHGI et al.

Skeletal Muscle Mechanics from Hill-Based Muscle Model to Computer Applications: State of the Art Rev...

that the maximum isometric strength of the selected muscles and the number of muscles in the model were parameters that greatly influenced the dynamic simulation results. They believe that as the physiological criteria were completely individual, more research should be done to ensure that the customization in musculoskeletal modeling was not sufficient and that muscle strengths during walking were predicted with high accuracy using multi-body models [44]. Table 1 presents a brief summary of simulation studies.

Table 1: *Studies on skeletal muscle*

Ref.	Visual	Structure	Method	Boundary conditions	Description
[7]		Muscle, bone, tendon, ligament and joint	Computer-based software	Rigid body assumption to obtain three-dimensional human body segment motion	Real-time monitoring during exercise has shown that muscles protect against the harmful effects of exercise.
[8]		Muscle	Nonlinear continuity mechanics	Piola-Kirchhoff stress tensor and Green-Lagrange strain tensor	A muscle model had constructed that could be applied to programs using the finite element method.
[10]		Denervated muscle	Finite element method	(Bidomain) model	Responses had studied due to changes in fiber parameters by simulations such as Hatchkin-Huxley.
[12]		Skeletal muscle and New Zealand white rabbit tibialis anterior muscle	Finite element method	Helmholtz free energy function	A visco-hyperelastic model had developed to describe the behavior of skeletal muscles under high pressure and to study muscle tissue.
[23]		Muscle, tendons and joints	Difference index calculation	Assuming that muscle increases strength and when the joint rotates as a trigonometric sine function was reduced	Muscle structure and basic muscle function had assessed.

DERESHGI et al.

Skeletal Muscle Mechanics from Hill-Based Muscle Model to Computer Applications: State of the Art Rev...

[25]		Muscle, bone, ligament and tendon	Finite element method	Assumption of constant cross-sectional stress for muscle length and calculation of moment arm	Constant cross-sectional stress assumption for muscle length and moment arm calculation.
[26]		Upper extremity muscles, tendons and joints	Musculoskeletal modeling package	15 degrees of freedom that defines the kinematics of the shoulder, elbow, forearm, wrist, thumb and index finger	A three-dimensional model had designed that included all the major muscles of the upper limb and characterized mechanical movement.
[29]		Brachialis muscle	Forward and inverse dynamic analysis	MR (at time t = 0) with motor units in the rest compartment = 100%.	The muscle fatigue model had developed based on the history of strength production of each muscle that could work with Hill muscle models.
[30]		Quadriceps tendons and patellar ligaments	Harvest technique and uniaxial tensile-fracture tests	16 tendons and ligaments with 10 mm wide, 200 cycles from 50 N – 800 N at 0.5 Hz	The mechanical tensile properties of the quadriceps tendons and patellar ligaments had analyzed.
[46]		Muscle	3D muscle modeling (LabVIEW program)	L_0: The length at which the muscle could produce the maximum active force	To investigate the deformation of the plate, transverse tension had applied to muscles of different lengths using isometric force.

3   Animal Studies

3.1   Experimental Studies

Lieber and Friden (1993) determined the effects of force on the tension created by the anterior muscles of the rabbit tibialis. They investigated the contractile properties of muscles using a light microscope

DERESHGI et al.

Skeletal Muscle Mechanics from Hill-Based Muscle Model to Computer Applications: State of the Art Rev...

after eccentric contraction, together with mechanical factors affecting muscle damage. They observed that the magnitude of the strain had a significant effect on the occurrence of muscle damage, and the strain timing had no significant effect. Contrary to popular belief, they concluded that after the eccentric contraction occurs, not only high strength but also the magnitude of active tension significantly affected muscle damage [45].

Donkelaar et al. (1999) to investigate the model acceptance of plane stress-strain studied the two-dimensional (transverse and longitudinal) surface deformation and stretching of the skeletal muscle. Therefore, they fabricated three-dimensional measurements by applying power signals to different muscle lengths. They observed that the muscle length did not affect the 11% strain perpendicular to the muscle surface. They also concluded that muscle fibers were smoothed when comparing stresses due to isometric two-dimensional contractions [46].

Felder et al. (2005) using the mouse hind link muscles as a model, measured the sarcomere length of the tibialis anterior (TA), extensor digitorum longus (EDL), and soleus muscles; also adjusted the ankle joints to angles ranging from 30° to 150°, to determine whether fiber length can be accurately normalized with high resolution. When the foot was in plantar flexion, they observed that TA and EDL fiber length increased significantly while soleus fiber length decreased, so they concluded that the crude fiber length was largely dependent on the tibiotarsal angle. Consequently, they statistically confirmed the use of sarcomere length to normalize fiber length [47].

3.2   Design, Modelling and Simulation Studies

Zuurbier et al. (1994) examined the length-force characteristics of aponeurosis in the passive, active, and isolated states. They used a two-factor analysis of variance to compare data. Relative elongation; 14.3% for the entire aponeurosis, 9.8% for the closest aponeurosis (25%), 3-5% for the middle of the aponeurosis (50%) and 52.3% for the furthest aponeurosis (25%). They observed that when active compared to passive and isolated states, the length of aponeurosis, affecting aponeurosis strength, was shorter in the range of 0.3 - 1.0 N and there was no difference in length between passive and isolated states. Consequently, they concluded that aponeurosis is heterogeneously distributed along the extension length [48].

Shue and Crago (1998) explained the muscular behavior according to length and velocity connections during constant and random stimulation by creating muscle-tendon Hill-type structure with a non-linear method based on the past and not related to the past. According to the results, the historical model performed well under all test conditions. They concluded that the stress-length relationship can be assessed closer to the correct result during constant stimulation and dynamic properties can be assessed during random stimulation [49].

Bourne et al. (2004) found a way to achieve a more realistic result by modeling trabecular tissue diversity using homogeneous and inhomogeneous finite element methods. Therefore, they examined tissue properties with CT scans. When the non-homogeneous finite element method was used, compared to the homogeneous finite element method, 13% more accurate results were obtained [50].

Loerakker et al. (2010) using MRI techniques and special finite element modeling, investigated the effects of time of exposure and intermittent load reduction on muscle tissue damage caused by deformation. They observed that 2-hour loading caused more damage than 10-minute loading, and temporary load relief at 2-minute intervals during 2-hour loading did not provide damage reduction [51].

4   Conclusion

Classical mechanics approach and finite element models used for mechanical analysis for muscles. Thus, force generation and power generation of muscles have been estimated. Although mechanical properties of muscles such as force, power and work are well known, more research should be done on muscle fatigue, muscle atrophy and viscoelasticity of muscle. In this way, the biochemical properties of the muscles will be better understood.

DERESHGI et al.

Skeletal Muscle Mechanics from Hill-Based Muscle Model to Computer Applications: State of the Art Rev...

5 Declarations

5.1 Study Limitations

None.

5.2 Acknowledgements

None.

5.3 Funding source

None.

5.4 Competing Interests

The authors declare that they have no known competing financial interests or personal relationships that could have appeared to influence the work reported in this paper.

References

[1] Serbest, K., & Eldoğan, O. (2014). Structure and biomechanics of skeletal muscle. *Academic Platform Journal of Engineering and Science*, *2*(3), 41-51.

[2] Hill, A. V. (1938). The heat of shortening and the dynamic constants of muscle. *Proceedings of the Royal Society of London. Series B-Biological Sciences*, *126*(843), 136-195.

[3] Hill, A. V. (1964). The effect of load on the heat of shortening of muscle. *Proceedings of the Royal Society of London. Series B. Biological Sciences*, *159*(975), 297-318.

[4] Huxley, A. F. (1957). Muscle structure and theories of contraction. *Prog. Biophys. Biophys. Chem*, *7*, 255-318.

[5] Huxley, A. F., & Simmons, R. M. (1971). Proposed mechanism of force generation in striated muscle. *Nature*, *233*(5321), 533-538.

[6] Feldman, A. G., Adamovich, S. V., Ostry, D. J., Flanagan, J. R., Winters, J., & Woo, S. L. Y. (1990). Multiple muscle systems: Biomechanics and movement organization.

[7] Chao, E. Y. S., Lynch, J. D., & Vanderploeg, M. J. (1993). Simulation and animation of musculoskeletal joint system.

[8] Johansson, T., Meier, P., & Blickhan, R. (2000). A finite-element model for the mechanical analysis of skeletal muscles. *Journal of Theoretical Biology*, *206*(1), 131-149.

[9] Zhao, J., & Narwani, G. (2005, June). Development of a human body finite element model for restraint system R&D applications. In *The 19th International Technical Conference on the Enhanced Safety of Vehicles (ESV), Paper* (No. 05-0399).

[10] Martinek, J., Stickler, Y., Reichel, M., Mayr, W., & Rattay, F. (2008). A Novel Approach to Simulate Hodgkin–Huxley-like Excitation With COMSOL Multiphysics. *Artificial Organs*, *32*(8), 614-619.

[11] Bai, X., Wei, G., Ye, M., Wang, D., Hu, Y., Liu, Z., ... & Wang, C. (2008, May). Finite element musculoskeletal modeling of mechanical virtual human of China. In *2008 2nd International Conference on Bioinformatics and Biomedical Engineering* (pp. 1847-1850). IEEE.

[12] Lu, Y. T., Zhu, H. X., Richmond, S., & Middleton, J. (2010). A visco-hyperelastic model for skeletal muscle tissue under high strain rates. *Journal of Biomechanics*, *43*(13), 2629-2632.

[13] Kocbach, J., Folgerø, K., Mohn, L., & Brix, O. (2011). A simulation approach to optimizing performance of equipment for thermostimulation of muscle tissue using COMSOL multiphysics. *Biophysics and Bioengineering Letters*, *4*(2), 9-33.

[14] Trinler, U., & Baker, R. (2018). Estimated landmark calibration of biomechanical models for inverse kinematics. *Medical Engineering & Physics*, *51*, 79-83.

[15] Lieber, R. L., Fazeli, B. M., & Botte, M. J. (1990). Architecture of selected wrist flexor and extensor muscles. *The Journal of Hand Surgery*, *15*(2), 244-250.

[16] Lieber, R. L., Loren, G. J., & Fridén, J. (1994). In vivo measurement of human wrist extensor muscle sarcomere length changes. *Journal of Neurophysiology*, *71*(3), 874-881.

DERESHGI et al.

Skeletal Muscle Mechanics from Hill-Based Muscle Model to Computer Applications: State of the Art Rev...

[17] Rotter, N., Tobias, G., Lebl, M., Roy, A. K., Hansen, M. C., Vacanti, C. A., & Bonassar, L. J. (2002). Age-related changes in the composition and mechanical properties of human nasal cartilage. *Archives of Biochemistry and Biophysics*, *403*(1), 132-140.

[18] Lehtinen, J., Tingart, M., Apreleva, M., Zurakowski, D., Palmer, W., & Warner, J. (2003). Practical assessment of rotator cuff muscle volumes using shoulder MRI. *Acta Orthopaedica Scandinavica*, *74*(6), 722-729.

[19] Mochizuki, T., Sugaya, H., Uomizu, M., Maeda, K., Matsuki, K., Sekiya, I., ... & Akita, K. (2008). Humeral insertion of the supraspinatus and infraspinatus: new anatomical findings regarding the footprint of the rotator cuff. *JBJS*, *90*(5), 962-969.

[20] Li, K., Wei, N., Cheng, M., Hou, X., & Song, J. (2018). Dynamical coordination of hand intrinsic muscles for precision grip in diabetes mellitus. *Scientific Reports*, *8*(1), 1-13.

[21] Zilov, V. G., Khadartsev, A. A., Ilyashenko, L. K., Eskov, V. V., & Minenko, I. A. (2018). Experimental analysis of the chaotic dynamics of muscle biopotentials under various static loads. *Bulletin of Experimental Biology and Medicine*, *165*(4), 415-418.

[22] Zhang, N., Wei, N., & Li, K. (2020, July). Dynamic Analysis of Muscle Coordination at Different Force Levels during Grip and Pinch with Multiplex Recurrence Network. In *2020 42nd Annual International Conference of the IEEE Engineering in Medicine & Biology Society (EMBC)* (pp. 3788-3791). IEEE.

[23] Lieber, R. L. (1993). Skeletal muscle architecture: implications for muscle function and surgical tendon transfer. *Journal of Hand Therapy*, *6*(2), 105-113.

[24] Lee, T. Y., Sum, Y. N., Lin, Y. C., Lin, L., & Lee, C. (1999). Three-dimensional facial model reconstruction and plastic surgery simulation. *IEEE Transactions on Information Technology in Biomedicine*, *3*(3), 214-220.

[25] Teran, J., Sifakis, E., Blemker, S. S., Ng-Thow-Hing, V., Lau, C., & Fedkiw, R. (2005). Creating and simulating skeletal muscle from the visible human data set. *IEEE Transactions on Visualization and Computer Graphics*, *11*(3), 317-328.

[26] Holzbaur, K. R., Murray, W. M., & Delp, S. L. (2005). A model of the upper extremity for simulating musculoskeletal surgery and analyzing neuromuscular control. *Annals of Biomedical Engineering*, *33*(6), 829-840.

[27] Blemker, S. S., Pinsky, P. M., & Delp, S. L. (2005). A 3D model of muscle reveals the causes of nonuniform strains in the biceps brachii. *Journal of Biomechanics*, *38*(4), 657-665.

[28] Rehorn, M. R., & Blemker, S. S. (2010). The effects of aponeurosis geometry on strain injury susceptibility explored with a 3D muscle model. *Journal of Biomechanics*, *43*(13), 2574-2581.

[29] Silva, M. T., Pereira, A. F., Martins, J. M., & Biomechatronics Research Group. (2011). An efficient muscle fatigue model for forward and inverse dynamic analysis of human movements. *Procedia IUTAM*, *2*, 262-274.

[30] Stäubli, H. U., Schatzmann, L., Brunner, P., Rincón, L., & Nolte, L. P. (1999). Mechanical tensile properties of the quadriceps tendon and patellar ligament in young adults. *The American Journal of Sports Medicine*, *27*(1), 27-34.

[31] Bayraktar, H. H., Morgan, E. F., Niebur, G. L., Morris, G. E., Wong, E. K., & Keaveny, T. M. (2004). Comparison of the elastic and yield properties of human femoral trabecular and cortical bone tissue. *Journal of Biomechanics*, *37*(1), 27-35.

[32] Ward, S. R., Eng, C. M., Smallwood, L. H., & Lieber, R. L. (2009). Are current measurements of lower extremity muscle architecture accurate?. *Clinical Orthopaedics and Related Research*, *467*(4), 1074-1082.

[33] Alexander, N., & Schwameder, H. (2016). Lower limb joint forces during walking on the level and slopes at different inclinations. *Gait & Posture*, *45*, 137-142.

[34] Alexander, N., & Schwameder, H. (2016). Effect of sloped walking on lower limb muscle forces. *Gait & Posture*, *47*, 62-67.

[35] Trinler, U., Schwameder, H., Baker, R., & Alexander, N. (2019). Muscle force estimation in clinical gait analysis using AnyBody and OpenSim. *Journal of biomechanics*, *86*, 55-63.

DERESHGI et al.

Skeletal Muscle Mechanics from Hill-Based Muscle Model to Computer Applications: State of the Art Rev...

[36] Brekelmans, W. A. M., Poort, H. W., & Slooff, T. J. J. H. (1972). A new method to analyse the mechanical behaviour of skeletal parts. *Acta Orthopaedica Scandinavica*, *43*(5), 301-317.

[37] Delp, S. L., Ringwelski, D. A., & Carroll, N. C. (1994). Transfer of the rectus femoris: effects of transfer site on moment arms about the knee and hip. *Journal of Biomechanics*, *27*(10), 1201-1211.

[38] Anderson, D. L. (1996, March). Role of rapid prototyping in preoperative planning and patient-specific implant generation. In *Proceedings of the 1996 Fifteenth Southern Biomedical Engineering Conference* (pp. 558-559). IEEE.

[39] Godest, A. C., Beaugonin, M., Haug, E., Taylor, M., & Gregson, P. J. (2002). Simulation of a knee joint replacement during a gait cycle using explicit finite element analysis. *Journal of Biomechanics*, *35*(2), 267-275.

[40] Helwig, P., Faust, G., Hindenlang, U., Kröplin, B., & Eingartner, C. (2006). Finite element analysis of a bone-implant system with the proximal femur nail. *Technology and Health Care*, *14*(4-5), 411-419.

[41] Cilingir, A. C., Ucar, V., & Kazan, R. (2007). Three-dimensional anatomic finite element modelling of hemi-arthroplasty of human hip joint. *Trends Biomater Artif Organs*, *21*(1), 63-72.

[42] Linder-Ganz, E., Shabshin, N., Itzchak, Y., & Gefen, A. (2007). Assessment of mechanical conditions in sub-dermal tissues during sitting: a combined experimental-MRI and finite element approach. *Journal of Biomechanics*, *40*(7), 1443-1454.

[43] Carbone, V., van der Krogt, M. M., Koopman, H. F., & Verdonschot, N. (2016). Sensitivity of subject-specific models to Hill muscle–tendon model parameters in simulations of gait. *Journal of Biomechanics*, *49*(9), 1953-1960.

[44] Żuk, M., Syczewska, M., & Pezowicz, C. (2018). Influence of uncertainty in selected musculoskeletal model parameters on muscle forces estimated in inverse dynamics-based static optimization and hybrid approach. *Journal of Biomechanical Engineering*, *140*(12).

[45] Lieber, R. L., & Friden, J. (1993). Muscle damage is not a function of muscle force but active muscle strain. *Journal of Applied Physiology*, *74*(2), 520-526.

[46] Van Donkelaar, C. C., Willems, P. J. B., Muijtjens, A. M. M., & Drost, M. R. (1999). Skeletal muscle transverse strain during isometric contraction at different lengths. *Journal of Biomechanics*, *32*(8), 755-762.

[47] Felder, A., Ward, S. R., & Lieber, R. L. (2005). Sarcomere length measurement permits high resolution normalization of muscle fiber length in architectural studies. *Journal of Experimental Biology*, *208*(17), 3275-3279.

[48] Zuurbier, C. J., Everard, A. J., van der Wees, P., & Huijing, P. A. (1994). Length-force characteristics of the aponeurosis in the passive and active muscle condition and in the isolated condition. *Journal of Biomechanics*, *27*(4), 445-453.

[49] Shue, G. H., & Crago, P. E. (1998). Muscle–tendon model with length history-dependent activation–velocity coupling. *Annals of Biomedical Engineering*, *26*(3), 369-380.

[50] Bourne, B. C., & van der Meulen, M. C. (2004). Finite element models predict cancellous apparent modulus when tissue modulus is scaled from specimen CT-attenuation. *Journal of Biomechanics*, *37*(5), 613-621.

[51] Loerakker, S., Stekelenburg, A., Strijkers, G. J., Rijpkema, J. J. M., Baaijens, F. P. T., Bader, D. L., ... & Oomens, C. W. J. (2010). Temporal effects of mechanical loading on deformation-induced damage in skeletal muscle tissue. *Annals of Biomedical Engineering*, *38*(8), 2577-2587.